Neurobiology of Disease

Regulation of Cu/Zn-Superoxide Dismutase Expression via the Phosphatidylinositol 3 Kinase/Akt Pathway and Nuclear Factor-κB

Ana I. Rojo, Marta Salinas, Daniel Martín, Rosario Perona, and Antonio Cuadrado

Institute of Biomedical Investigation and Department of Biochemistry, Faculty of Medicine, Autónoma University of Madrid, 28029 Madrid, Spain

Aerobic cells adjust the expression of antioxidant enzymes to maintain reactive oxygen species within tolerable levels. In addition, phosphatidylinositol 3 kinase (PI3K) and its downstream protein kinase effector Akt adapt cells to survive in the presence of oxidative stress. Here we provide evidence for an association between these two defense systems via transcriptional regulation of Cu/Zn-superoxide dismutase (Cu/Zn-SOD). PC12 pheochromocytoma cells expressing active Akt1 exhibit lower ROS levels in response to hydrogen peroxide, as determined with the superoxide-sensitive probe hydroethidine. Transfection of constitutive or 4-hydroxytamoxifen-inducible versions of Akt1 results in higher messenger RNA and protein levels of Cu/Zn-SOD. Luciferase reporter constructs, carrying different length fragments of the human *sod1* gene promoter, have identified a region between –552 and –355 that is targeted by PI3K and Akt and that contains a putative site of regulation by nuclear factor-κB (NF-κB). Nerve growth factor (NGF) and Akt augment the transactivating activity and produce higher nuclear levels of p65-NF-κB. Electrophoretic mobility shift assays indicate that the putative NF-κB regulatory sequence binds p65-NF-κB more efficiently in nuclear extracts from these cells. A dominant-negative mutant of IκBα further demonstrates that the PI3K/Akt axis targets the *sod1* promoter at the level of the newly characterized NF-κB site. These results illustrate a new mechanism by which the PI3K/Akt pathway protects cells against oxidative stress, involving the upregulation of Cu/Zn-SOD gene expression, and the results identify NF-κB as a key mediator in the regulation of this gene.

Key words: **superoxide dismutase; PI3K; Akt; NF-κB; oxidative stress; reactive oxygen species; hydrogen peroxide**

Introduction

Reactive oxygen species (ROS) are generated during aerobic metabolism or in response to external toxins and produce oxidative damage to cellular macromolecules (Klein and Ackerman, 2003). Adaptive responses adjust the abundance and activity of antioxidant systems to cellular needs (Fridovich, 1999). One such system is constituted by the superoxide dismutase (SOD) enzymes, which convert superoxide anion into molecular oxygen and hydrogen peroxide (H_2O_2) (Fridovich, 1997; Zelko et al., 2002).

Cu/Zn-SOD, the most abundant and ubiquitous isoform, may have great physiological significance and therapeutic potential in neurodegenerative diseases because the CNS is particularly sensitive to oxidant injury. For instance, an inverse correlation has been reported between Cu/Zn-SOD activity and neuronal death after acute brain injury (Takeuchi et al., 2000). Moreover, the level of Cu/Zn-SOD mRNA was reduced significantly in the substantia nigra of marmosets treated with the parkinsonian toxin MPTP (1-methyl-4-phenyl-1,2,3,6-tetrahydropyridine) and in patients with Parkinson's disease (Kunikowska and Jenner, 2003). In addition, Cu/Zn-SOD transgenic mice were protected against the neurotoxic effects of 6-hydroxydopamine (6-OHDA) (Asanuma et al., 1998). Transcription of *sod1*, the gene coding for Cu/Zn-SOD, is regulated tightly in response to diverse stimuli, including stress, proinflammatory cytokines, and growth factors (Kong et al., 1993; Yoo et al., 1999; Chang et al., 2002; Park and Rho, 2002). However, despite the detailed characterization of the regulatory promoter region, little is known about the intracellular signaling cascades that govern *sod1* expression.

The phosphatidylinositol 3 kinase (PI3K) and its best characterized effector, the Ser/Thr protein kinase Akt/protein kinase B (PKB), exert antioxidant effects in central and peripheral neurons (Brunet et al., 2001; Franke et al., 2003). Recently, we have reported the protective effect of active Akt1 against peptides of β-amyloid protein (Martin et al., 2001), against the Parkinson-inducing toxins 1-methyl-4-phenylpyridinium (MPP^+) (Salinas et al., 2001) and 6-OHDA (Salinas et al., 2003), and against apoptotic concentrations of H_2O_2 (Martin et al., 2002). In these cases, expression of a constitutively active version of Akt1 prevented the increase in ROS that follows treatment of PC12 cells with these neurotoxins. Despite these reports, a direct regulatory role of this pathway on the canonical antioxidant defenses such as Cu/Zn-SOD has not been demonstrated clearly.

The survival effect of PI3K and Akt generally is attributed to Akt-mediated phosphorylation of proapoptotic proteins but also to transcription-dependent mechanisms (Kuruvilla et al., 2000;

Received Feb. 12, 2004; revised July 1, 2004; accepted July 7, 2004.

This work was supported by Grants SAF2001-0545 from Ministry of Science and Technology and 08.5/0048/2001 from Comunidad Autónoma of Madrid. We thank Beatriz Palacios for her excellent technical assistance.

Correspondence should be addressed to Dr. Antonio Cuadrado, Department of Biochemistry, Autónoma University of Madrid, Arzobispo Morcillo 4, 28029 Madrid, Spain. E-mail: antonio.cuadrado@uam.es.

DOI:10.1523/JNEUROSCI.2111-04.2004

 0270-6474/04/247324-11$15.00/0

Brunet et al., 2001). Several transcription factors have been identified as substrates of Akt that might mediate Akt actions on gene expression of antioxidant enzymes. Akt directly phosphorylates the Forkhead transcription factors of the FOXO class (Brunet et al., 1999) and may participate in the activation of cAMP response element binding protein (CREB) (Du and Montminy, 1998) and nuclear factor-κB (NF-κB) (Kane et al., 1999).

In this study we report that the PI3K/Akt axis upregulates the expression of Cu/Zn-SOD via the activation of NF-κB. These data contribute to reveal the mechanism whereby PI3K/Akt provide protection against oxidative injury and suggest a new therapeutic strategy to increase the antioxidant capacity of neurons via the activation of this survival pathway.

Materials and Methods

Cell culture and reagents. Rat pheochromocytoma PC12 cells [gift of Dr. H. Kleinman, National Institute of Dental and Craniofacial Research (NIDCR), National Institutes of Health (NIH), Bethesda, MD] were grown in DMEM supplemented with 7.5% heat-inactivated fetal bovine serum, 7.5% heat-inactivated horse serum, and 80 μg/ml gentamycin. PC12 cells stably expressing myr-Akt1-ER* were grown in medium supplemented with serum treated with charcoal-coated dextran (Sigma–Aldrich, Madrid, Spain). Stable transfections with the expression vectors pCEFL(X$^-$)EGFP, pCEFL(X$^-$)myr-EGFP-Akt1, and pcDNA3-myr-Akt1-ER* were made with SuperFect transfection reagent (Qiagen, Valencia, CA) according to the manufacturer's instructions. Transfected cells were selected in 0.5 mg/ml G418. Other reagents were nerve growth factor (NGF) (Promega, Madison, WI), H_2O_2, glutathione, LY294002, and 4-hydroxytamoxifen (4-HT; Sigma–Aldrich).

Plasmids. Constructs expressing the EGFP-Akt1 fusion proteins were generated as previously described (Salinas et al., 2001). For generation of pcDNA3-myr-Akt-ER*, the *Bam*HI/*Eco*RI fragment of pBluescript KS$^+$MER (Littlewood et al., 1995) was subcloned in the same sites of pcDNA3.myr-Akt1 (Salinas et al., 2000). This fragment comprises a mutant hormone-binding domain of the estrogen receptor (ER*) that does not bind β-estradiol but retains responsiveness to the synthetic steroid 4-HT. Then we put myr-Akt1 and ER* in the same reading frame and removed the stop codon of myrAkt1 by using a PCR strategy (details available on request). Expression vectors for anchored membrane forms of myristoylated Akt1 and farnesylated PI3K included the following: pcDNA3-myr-EGFP-Akt1 (Salinas et al., 2000), pSG5gag-Akt1, and pSG5p110α-PI3K-CAAX (gift of Dr. J. Downward, Imperial Cancer Research Fund, London, UK). From pSG5p110α-PI3K-CAAX the *Eco*RI fragment containing the coding sequence for PI3K-CAAX was subcloned into vector pTG6600 under the control of the CMV promoter; pCMV-m1, expressing the muscarinic m1 receptor, was a gift of Dr. S. Gutkind (NIDCR, NIH, Bethesda, MD); NF-κB-HIV contains the NF-κB site of the HIV enhancer/promoter (Montaner et al., 1999). Other expression vectors were double-point mutant IκBα(S32A/S36A) (Traenckner et al., 1995) and pGal4-p65 and pGal4-LUC (Montaner et al., 1999; Madrid et al., 2000). Deletion mutants from the 5′ flanking region of *sod1* were generated by following the same strategy described in Minc et al. (1999). Briefly, PCR fragments of different lengths were amplified from the 5′-flanking region of the human *sod1* gene by using *Taq* Gold DNA polymerase (Promega). For amplification of fragments –1499, –952, –750, and –552, human genomic DNA was used as template, and a common reverse primer was used (5′-CCGA*AAGCTT*GAGACTACGACGC-AAACCCAG-3′) with a *Hind*III site to facilitate subsequent cloning. Forward oligonucleotides were designed according to the size of the future fragment: –1499 bp, 5′-CCGA*CTCGAG*CCCTTGGCAAGTTTA-CAATG-3′; –952 bp, 5′-CCGA*CTCGAG*GTGGTCCCAGGTACTT-GGGGA-3′; –750 bp, 5′-CCGA*CTCGAG*TATTTCCCTTGAAAGG-TAAG-3′; –552 bp, 5′-CCGA*CTCGAG*ACCGAATTCTGCCAACC-AAA-3′. A *Xho*I site was introduced in all forward primers to allow directional cloning into the reporter vector pGL3basic (Promega). Amplifications were performed by using 20 ng, with a thermal profile of (1) 96°C, 3 min; (2) 96°C, 2 min; (3) 65°C, 2 min; (4) 72°C, 3 min; (5) 40× to 2; (6)72°C, 5 min. The amplified fragments were introduced in pGL3basic between the *Xho*I and *Hind*III sites. PCR fragments –355, –157, –71, and –29 were amplified by using plasmid pGL3basic-*sod1*-1499 as template and the reverse primer 5′-ATAGGATCTCTG-*GCATGC*GAGAATCTCACG-3′, in which an *Sph*I is introduced to allow subsequent cloning. Forward oligonucleotides included the following: –355 bp, 5′-CCGA*CTCGAG*TGGCCAAACTCAGTCATAAC-3′; –157 bp, 5′-CCGA*CTCGAG*ACGCGCCCCTTGCCCCGCCC-3′; –71 bp, 5′-CCGAA*CTCGAG*ATTGGTTTGGGGCCAGAGTG-3′; and –29 bp, 5′-CCGA*CTCGAG*TATAAAGTAGTCGCGGAGAC-3′. The amplified fragments were subcloned in pGL3basic between sites *Xho*I and *Sph*I. NF-κB-*sod1* and NF-κB-*mut* were obtained with the following oligonucleotides: 5′-CTAGCAAA*GGTAAGTCCC*GGATCCAAA*GGTAAGTC-CC*GGATCAA*GGTAAGCCC*GGC-3′ and 5′-CTAGCAAAGGTAAGT-ATTGTCGACAAAGGTAAGTTACGGATCAAGGTAAGTATTGGC-3′ (underlined sites, NF-κB). These oligonucleotides were subcloned into *Nhe*I and *Xho*I sites of the minimal *sod1* promoter pGL3basic-*sod1*-29.

Luciferase assays. PC12 cells were seeded in 24-well plates (75,000 cells per well), cultured for 16 hr, and transfected with a DNA mixture consisting of 100 ng of the appropriate luciferase construct and 400 ng of the effector plasmid or empty vector, using Lipofectamine reagent (Invitrogen, Carlsbad, CA) according to the manufacturer's recommendations. After 24 hr from transfection the cells were serum-starved for 16 hr, lysed, and assayed for luciferase activity with the Luciferase Assay System (Promega) according to the manufacturer's instructions; relative light units were measured in a BG1 Optocomp I, GEM Biomedical luminometer (Sparks, NV).

Analysis of mRNA levels by reverse transcriptase-PCR. Total cellular RNA was extracted with Trizol reagent (Invitrogen). Equal amounts (1 μg) of RNA from each treatment were reverse-transcribed (75 min, 42°C), using 5 U of avian myeloblastosis virus reverse transcriptase (RT) in the presence of 20 U of RNasin (Promega). cDNA amplification was performed in 25 μl of PCR buffer [containing (in mM): 10 Tris-HCl, 50 KCl, 5 $MgCl_2$, plus 0.1% Triton X-100, pH 9.0] containing 2.5 mM digoxigenin-dUTP, 0.6 U of *Taq* DNA polymerase (Promega), and 30 pmol of synthetic gene-specific primers for Cu^{2+}/Zn^{2+}-SOD (forward, 5′-TTCGAGCAGAAGGCAAGCGGTGAA-3′; reverse, 5′-AATCCCAA-TCACACCACAAGCCAA-3′). To ensure that equal amounts cDNA were added to the PCR, we amplified the β-actin housekeeping gene by using synthetic oligonucleotides (forward, 5′-TGTTTGAGACCTTCAA-CACC-3′; reverse, 5′-CGCTCATTGCCGATAGTGAT-3′). After an initial denaturation step (4 min at 94°C) the amplification of each cDNA was performed at the optimal number of cycles within linear range (data not shown), 19 cycles, using a thermal profile of 1 min at 94°C (denaturation), 1 min at 58°C (annealing), and 1 min at 72°C (elongation). The amplified PCR products were resolved in 1.8% agarose gel electrophoresis and transferred to nylon membranes (Biodyne, Pall Corporation, New York, NY). Chemiluminescence detection was performed with a digoxigenin luminescence detection kit (Roche Molecular Biochemicals, Basel, Switzerland).

Immunoblotting. The primary antibodies used were anti-Cu^{2+}/Zn^{2+}-SOD (StressGen, Victoria, British Columbia, Canada), anti-p65, anti-Sp1, anti-IκBα, and anti-Akt1C20 (Santa Cruz Biotechnology, Santa Cruz, CA); anti-phospho-Thr^{308}Akt1 (New England Biolabs, Beverly, MA); and anti-protein-disulfide-isomerase (gift from Dr. J. G. Castaño, Chief Advisor of Scientific Investigations, Institute of Biomedical Investigations, Autónoma University of Madrid). Cells were washed once with cold PBS and lysed on ice with 200 μl of lysis buffer [containing (in mM): 137 NaCl, 20 Tris-HCl, pH 7.5, 1 phenylmethylsulfonyl fluoride, 20 NaF, 1 sodium pyrophosphate, and 1 Na_3VO_4 plus 1% Nonidet P-40, 10% glycerol, 1 μg/ml leupeptin]. Precleared cell lysates were resolved in SDS-PAGE and transferred to Immobilon membranes (Millipore, Billerica, MA). These membranes were analyzed by using the primary antibodies indicated above and peroxidase-conjugated secondary antibodies. Proteins were detected by enhanced chemiluminescence (Pierce Biotechnology, Rockford, IL). Densitometric analyses of representative immunoblots were performed with NIH Image software (Bethesda, MD).

Flow cytometry. Intracellular ROS were detected with hydroethidine (HEt; Molecular Probes, Leiden, The Netherlands) (bandpass, 575/24

nm filter), using a FACScan flow cytometer (BD Biosciences, Madrid, Spain). Cells were detached from the plates, washed with PBS, incubated with 2 μM HEt for 1 hr at 37°C, and analyzed immediately. Baseline incorporation of the probe was determined in cells incubated in 2 μM HEt for 1 hr at 4°C. For Annexin-V-phycoerythrin (Annexin-V-PE) staining the cells were detached mechanically after treatments and washed twice with Annexin-V binding buffer [containing (in mM): 10 HEPES-NaOH, pH 7.4, 150 NaCl, 5 KCl, 1 $MgCl_2$, 1.8 $CaCl_2$]. Cells were resuspended in 100 μl of a 1:20 dilution of Annexin-V-PE (Bender MedSystems Diagnostics, Vienna, Austria) in Annexin-V binding buffer containing 2 μM 7-aminoactinomycin D (7-AAD) and were incubated for 15 min at room temperature. Fluorescence was measured with bandpass 620/22 and 575/24 nm filters. For immunostaining the cells were fixed with 4% paraformaldehyde for 1 hr at 4°C, washed with PBS, permeabilized with 0.2% Triton X-100 in PBS buffer for 5 min at 4°C, and incubated for 1 hr with anti-Cu/Zn-SOD (1:100) diluted in PBS and for 1 hr with Alexa 465-conjugated secondary antibody (1:500; Molecular Probes) in PBS.

Confocal microscopy. Cells were seeded on glass-bottom 35 mm plates (Willco, Amsterdam, The Netherlands) and incubated with 0.5 mM H_2O_2 for 3 hr and afterward with 2 μM HEt for 1 hr at 37°C. Confocal microscopy was performed via a Leica SP2 system (Nussloch, Germany). For HEt we used an excitation wavelength of 488 nm; fluorescence was detected at wavelengths between 557 and 740 nm. For Hoechst 33258 we used an excitation wavelength of 351 nm; fluorescence was detected at wavelengths between 386 and 512 nm.

Preparation of nuclear and cytosolic extracts. Cytosolic and nuclear fractions were prepared as previously described (Minc et al., 1999). Briefly, 5×10^6 cells were washed three times with cold PBS and harvested by centrifugation at 1100 rpm for 10 min. The cell pellet was resuspended carefully in three pellet volumes of cold buffer A [containing (in mM): 20 HEPES, pH 7.0, 0.15 EDTA, 0.015 EGTA, 10 KCl, 1 phenylmethylsulfonyl fluoride, 20 NaF, 1 sodium pyrophosphate, and 1 Na_3VO_4 plus 1% Nonidet P-40, 1 μg/ml leupeptin]. Then the homogenate was centrifuged at 500 × *g* for 5 min. The supernatant corresponding to the cytosolic fraction was resolved in SDS-PAGE and immunoblotted with anti-p65, anti-IκBα, or anti-PDI antibodies. The nuclear pellet was resuspended in five pellet volumes of cold buffer B [containing (in mM): 10 HEPES, pH 8.0, 0.1 EDTA, 1 phenylmethylsulfonyl fluoride, 20 NaF, 1 sodium pyrophosphate, and 1 Na_3VO_4 plus 25% glycerol, 0.1 M NaCl, 1 μg/ml leupeptin]. After centrifugation in the same conditions indicated above, the nuclei were resuspended in two pellet volumes of hypertonic cold buffer C [containing (in mM): 10 HEPES, pH 8.0, 0.1 EDTA, 1 phenylmethylsulfonyl fluoride, 20 NaF, 1 sodium pyrophosphate, and 1 Na_3VO_4 plus 25% glycerol, 0.4 M NaCl, 1 μg/ml leupeptin] and were incubated for 30 min at 4°C in a rotating wheel. Nuclear debris was removed by centrifugation at 900 × *g* for 20 min at 4°C; the supernatant was resolved in SDS-PAGE and immunoblotted with anti-p65 and anti-Sp1 antibodies.

Electrophoretic mobility shift assays. The double-stranded wild-type oligonucleotide used as an NF-κB probe was 5′-CTAGCAAA*GGTAAGTCCCGGATCCAAAGGTAAGTCCCGGATCAAGGTAAGTCCC*-GGC-3′ and for the mutant version was 5′-CTAGCAAAGGTAAGTAT TGTCGACAAAGGTAAGTTACGGATCAAGGTAAGTATTGGC-3′. Then 250 ng/μl of each oligonucleotide was annealed by incubation in STE buffer [containing (in mM): 100 NaCl, 10 Tris-HCl, pH 8.0, and 1 EDTA] at 80°C for 2 min. The mixture was cooled down slowly to 4°C, with a thermal profile of 1°C/min in a thermal incubator. Annealed oligonucleotides were diluted to 25 ng/μl in STE buffer. 5′-End labeling was performed with T4 polynucleotide kinase (Promega), using 25 ng of double-stranded oligonucleotide and 25 μCi [γ^{32}P]-ATP (3000 Ci/mmol; Amersham Biosciences, Buckinghamshire, UK). The labeled probes were purified in a G-25 spin column (Amersham Biosciences). The binding reaction mixture contained 5 μg of nuclear protein extract diluted in a buffer containing, at final concentration, 40 mM HEPES, pH 8.0, 50 mM KCl, 0.05% Nonidet P-40, 1% dithiothreitol, and 10 μg/ml poly(dI-dC) in a total volume of 20 μl. Antibody (2 μg) or unlabeled competitor probe (25 ng) was added, and the reaction was incubated for 1 hr at 25°C. Labeled DNA (0.25 ng) was added to the mixture and was submitted to an additional 20 min of incubation at 25°C. Samples were resolved at 4°C in a 5% nondenaturing polyacrylamide gel in 0.5× Tris-borate/EDTA buffer. After electrophoresis the gel was dried and autoradiographed.

Statistics. Student's *t* test was used to assess differences between groups. A p value < 0.05 was considered significant. Unless indicated, all experiments were performed at least three times with similar results. The values in the graphs correspond to the mean of at least three samples. Error bars indicate SD.

Results

To establish the conditions for analysis of ROS production under oxidative stress, we maintained PC12 cells in low-serum medium (1% fetal calf serum plus 1% horse serum) for 16 hr and then submitted the cells to 0.5 mM H_2O_2 for 3 hr. During the last hour of incubation the medium was supplemented with 2 μM HEt, a fluorescent probe most sensitive to anion superoxide, which with oxidation converts into ethidium and emits orange fluorescence (Bindokas et al., 1996; Chan et al., 1998). As shown in Figure 1*A*, counterstaining of these cells with the nuclear dye Hoechst 33258 and analysis by confocal microscopy evidenced HEt accumulation mostly in the nuclei of the cells submitted to oxidative damage. Then we quantified the incorporation of HEt by flow cytometry (Fig. 1*B*). Untreated cells exhibited a weak HEt incorporation. In contrast, H_2O_2 induced a significant increase in HEt fluorescence, consistent with the intracellular generation of ROS such as superoxide anion.

Next we analyzed the rate of HEt incorporation in PC12 cells submitted to H_2O_2 alone or in combination with reduced glutathione (GSH). As shown in Figure 1*C*, incubation with 0.5 mM H_2O_2 for >2 hr resulted in a three- to fourfold accumulation of HEt fluorescence. Moreover, the addition of 10 mM GSH 30 min before H_2O_2 treatment prevented the oxidation of HEt, as expected from its antioxidant properties.

To determine the role of the PI3K/Akt pathway in protection against ROS toxicity, we used PC12 cells stably transfected with expression vectors for enhanced green fluorescence protein (EGFP), as a control, or an Akt fusion protein, myr-EGFP-Akt1, containing EGFP at the N terminus of mouse Akt1 and a myristoylation signal that targets this chimera to the plasma membrane and confers constitutive activation (Salinas et al., 2001). Figure 2*A* shows the endogenous 59 kDa Akt protein and the ectopically expressed 85 kDa myr-EGFP-Akt1 fusion protein in EGFP- and myr-EGFP-Akt1-transfected cells, respectively. In addition, as shown in Figure 2*B*, when these cells were placed in low-serum medium for 16 hr and analyzed with antibodies that specifically recognize the phosphorylated, active form of Akt, we observed that only myr-EGFP-Akt1 retains activity (for a more detailed description of these constructs, see Salinas et al., 2001).

The presence of EGFP in the control cells or the EGFP moiety in the myr-EGFP-Akt1 cells allowed for analysis of single living cells by flow cytometry in combination with the orange fluorescence of HEt-stained cells. Cells maintained under low-serum conditions for 16 hr were submitted to several H_2O_2 concentrations for 3 hr and stained with HEt during the last hour. As shown in Figure 2*C*, in the EGFP cells H_2O_2 induced a three- to fourfold increase in the HEt fluorescence in a concentration range of 0.5–1 mM. Interestingly, the myr-EGFP-Akt1 cells exhibited a lower basal level of HEt fluorescence and were much more refractory to HEt incorporation in the presence of H_2O_2. These results indicate that activation of the PI3K/Akt pathway exerts antioxidant effects in PC12 cells.

In additional flow cytometry experiments, we confirmed that the antioxidant effects elicited by the PI3K/Akt pathway corre-

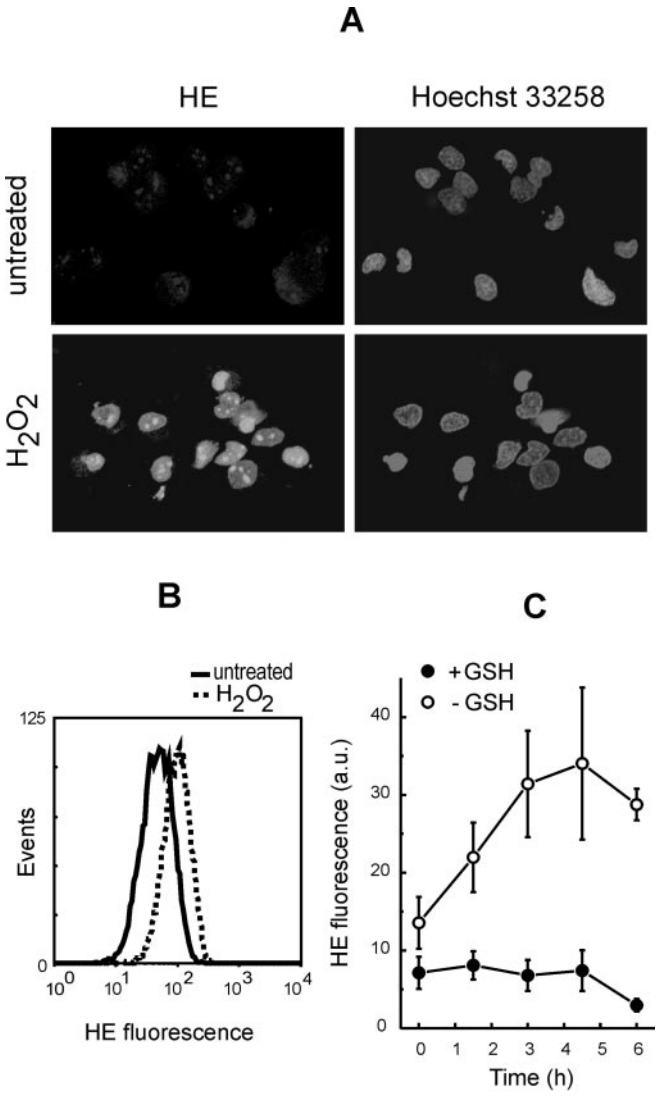

Figure 1. H_2O_2 increases intracellular ROS as determined by HEt staining. PC12 cells were maintained in low-serum conditions for 16 hr and then untreated or incubated with 0.5 mM H_2O_2 for 3 hr. During the last hour of the experiment, 2 μM HEt was added. *A*, Confocal microscopy pictures of representative fields from untreated and H_2O_2-treated cells stained with HEt (HE) and Hoechst 33258. *B*, Flow cytometry analysis of H_2O_2-induced intracellular ROS production in HEt-stained cells. A representative sample of 10,000 cells is shown for untreated or 0.5 mM H_2O_2-treated cells. *C*, Analysis by flow cytometry of the HEt incorporation rate in cells submitted to 0.5 mM H_2O_2 in the absence and in the presence of 10 mM GSH.

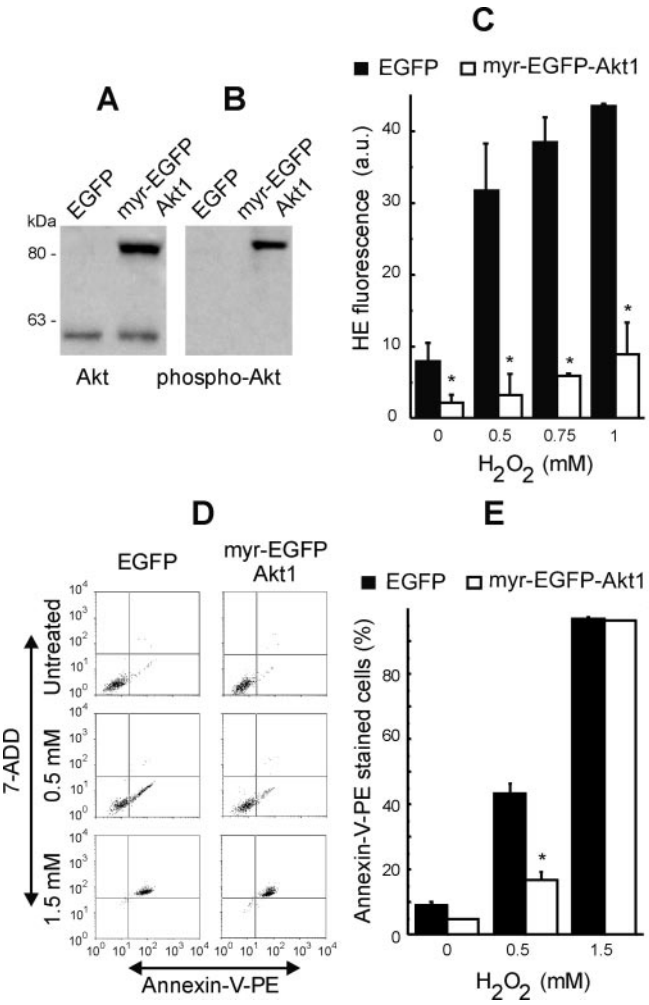

Figure 2. PC12 cells expressing active Akt1 exhibit oxidant and apoptotic protection. PC12 cells were stably transfected with expression vectors for EGFP or myr-EGFP-Akt1. *A*, Immunodetection of endogenous Akt and ectopically expressed myr-EGFP-Akt1 with anti-Akt antibodies. *B*, Immunodetection of active, phosphorylated Akt with anti-phospho-Akt antibodies. *C*, Flow cytometry determination of ROS in PC12 cells submitted for 3 hr to the indicated H_2O_2 concentrations as described in Figure 1; $^*p < 0.001$. *D*, Determination by flow cytometry of H_2O_2-induced apoptosis and necrosis in cells stained with Annexin-V-PE and 7-AAD. EGFP and myr-EGFP-Akt1 cells were treated with 0.5 or 1.5 mM H_2O_2 for 6 hr and then stained for 15 min with Annexin-V-PE (1:20 v/v) and 2 μM 7-AAD. A representative sample of 10,000 cells is shown for each experimental condition. *E*, Comparison of the percentages of dead cells, determined from Annexin-V-PE staining at the bottom right and top right quadrants in *D*, which represent the total number of cells in apoptosis and necrosis. $^*p < 0.001$, comparing H_2O_2-treated EGFP and myr-EGFP-Akt1 groups.

lated with protection against ROS-induced apoptosis. We analyzed exposure of phosphatidylserine on the outer plasma membrane leaflet as an early hallmark of apoptosis. This alteration was analyzed with Annexin-V-PE. To discriminate apoptosis from necrosis, we stained the cells simultaneously with the red fluorescent vital dye 7-AAD, which enters cells lacking membrane integrity and, therefore, allows for detection of necrotic cells (Hasper et al., 2000). EGFP and myr-EGFP-Akt1 cells were maintained under low-serum conditions for 16 hr and then were submitted to 0.5 or 1.5 mM H_2O_2 for 6 hr and finally were stained for 15 min with Annexin-V-PE and 7-AAD. As shown in Figure 2, *D* and *E*, in the absence of H_2O_2 most cells were Annexin-V-PE- and 7-AAD-negative, indicating that they were viable. After 0.5 mM H_2O_2 treatment ~40% of the EGFP cells were Annexin-V-PE-positive and 7-AAD-negative, indicating that this population was undergoing apoptotic cell death. In contrast, in the myr-EGFP-Akt1 cells this percentage was only ~20%. On the other hand, after 1.5 mM H_2O_2 treatment almost the entire populations of EGFP and myr-EGFP-Akt1 cells were stained with both 7-AAD and Annexin-V-PE. Therefore, these results indicate that the PI3K/Akt pathway attenuates ROS-induced apoptosis, but not necrosis.

Because the oxidant fluorescent probe used in this study, HEt, is most sensitive for anion superoxide, we analyzed whether Akt exerts its antioxidant effect via the activation of Cu/Zn-SOD. As shown Figure 3, *A* and *B*, the basal messenger RNA and protein levels of Cu/Zn-SOD were elevated significantly in myr-EGFP-Akt1 cells, suggesting that Akt upregulates Cu/Zn-SOD expression. Moreover, as shown in Figure 3*C*, flow cytometry analysis of EGFP and myr-EGFP-Akt1 cells immunostained with anti-Cu/

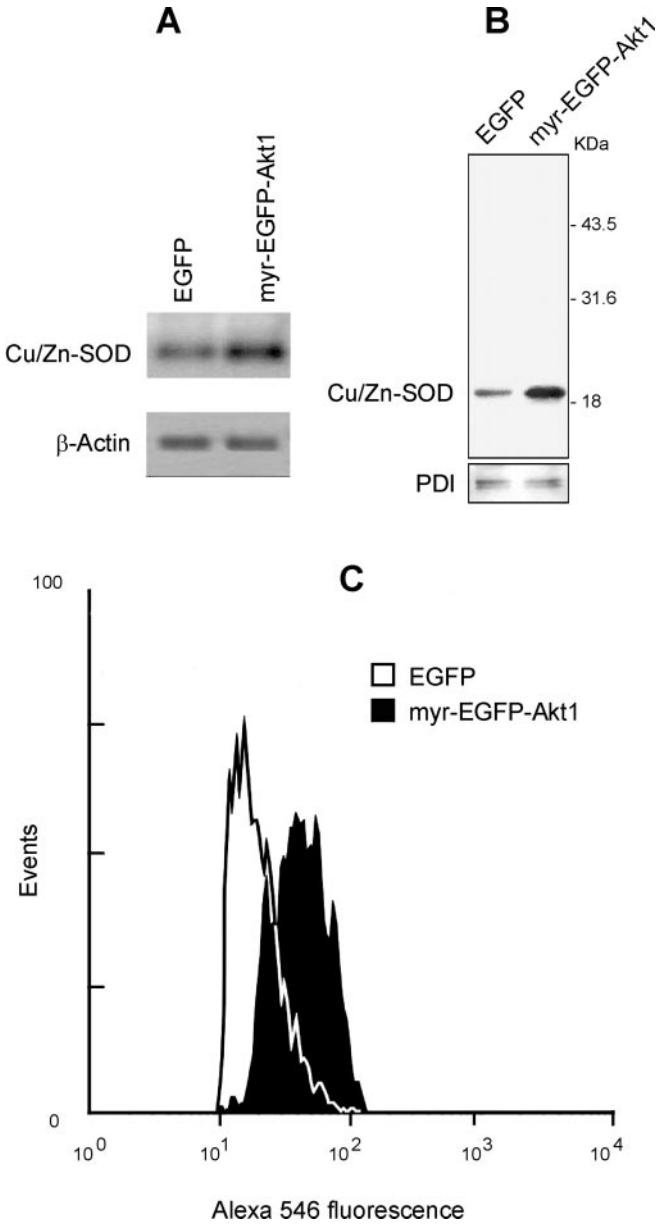

Figure 3. PC12 cells expressing active Akt1 exhibit higher levels of Cu/Zn-SOD messenger RNA and protein. *A*, Semi-quantitative RT-PCR of EGFP and myr-EGFP-Akt1 cells showing induction of Cu/Zn-SOD mRNA. Top, Cu/Zn-SOD mRNA; bottom, β-actin mRNA showing a similar amount of RNA per lane. *B*, Immunoblot showing the levels of Cu/Zn-SOD protein in the same cells. Top, Blot with anti-Cu/Zn-SOD antibodies; bottom, blot with anti-PDI antibodies showing a similar amount of protein per lane. *C*, Flow cytometry analysis of Cu/Zn-SOD protein levels in EGFP and myr-EGFP-Akt1 cells after fixation, permeabilization, and staining with anti-Cu/Zn-SOD antibodies.

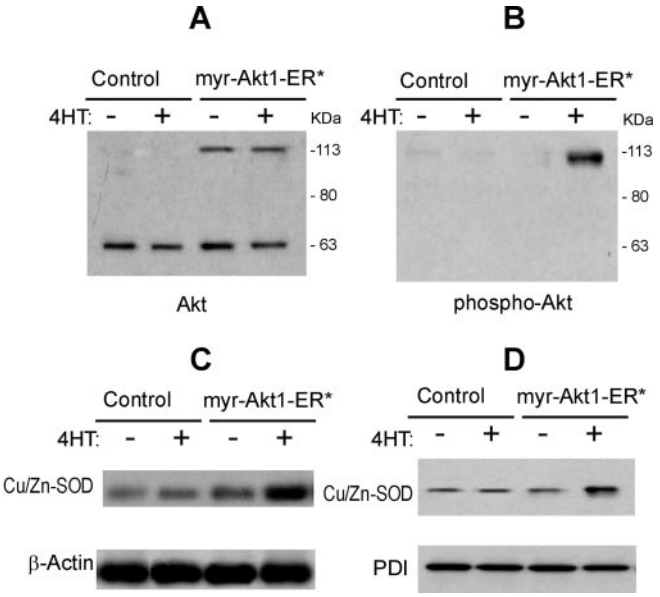

Figure 4. Analysis of Cu/Zn-SOD levels in PC12 cells expressing a conditionally active version of Akt1. PC12 cells, stably transfected with an expression vector for myr-Akt1-ER*, were submitted to 1 μM 4-HT for 16 hr under low-serum conditions. *A*, Immunodetection of endogenous Akt and ectopically expressed myr-Akt1-ER* with anti-Akt antibodies. *B*, Immunodetection of active, phosphorylated Akt with anti-phospho-Akt antibodies. *C*, Semi-quantitative RT-PCR of vector- and myr-Akt1-ER*-transfected cells showing the levels of Cu/Zn-SOD mRNA in the presence and absence of 4-HT. Top, Cu/Zn-SOD mRNA; bottom, β-actin mRNA showing a similar amount of RNA per lane. *D*, Immunoblot showing the levels of Cu/Zn-SOD protein in the same cells in the presence and absence of 4-HT. Top, Blot with anti-Cu/Zn-SOD antibodies; bottom, blot with anti-PDI antibodies showing a similar amount of protein per lane.

Zn-SOD antibodies indicated that the levels of this enzyme were increased two- to threefold in cells expressing active Akt1.

To confirm these observations further, we established a PC12 cell line transfected with an expression vector for a conditionally active chimera of Akt, myr-Akt1-ER*. In this protein the myristoylated Akt was fused at its C-terminal end with a mutated version of the hormone-binding domain from the estrogen receptor (see Materials and Methods). This fusion protein is expressed in an inactive form and becomes activated in the presence of 4-HT. Figure 4*A* shows the expression of endogenous 59 kDa Akt and the ectopically expressed 110 kDa fusion protein, and Figure 4*B* shows that the addition of 1 μM 4-HT resulted in the activation of this chimera as determined with activation-specific anti-phospho-Akt1 antibodies. Interestingly, as shown in Figure 4, *C* and *D*, when PC12 cells stably transfected with this construct were used to assess the levels of Cu/Zn-SOD, we observed that the addition of 4-HT for 16 hr induced the expression of both mRNA and protein of this antioxidant enzyme in the myr-Akt1-ER* cells and did not have a significant effect on control vector-transfected PC12 cells.

In a previous study we reported that H_2O_2 induces a transient activation of Akt but, in turn, results in inactivation and caspase 3-dependent and -independent degradation of Akt (Martin et al., 2002). For that reason we analyzed the kinetics of Akt phosphorylation/dephosphorylation and proteolytic degradation together with the changes in Cu/Zn-SOD protein levels (Fig. 5). Control EGFP-transfected cells exhibited a rise in phospho-Akt1 within minutes after 0.5 mM H_2O_2 stimulation, but no phosphorylated/active Akt was detected after 2 hr. In myr-EGFP-Akt1-transfected cells a drop in phospho-Akt1 also was detected, but, in contrast to control cells, a significant amount of phospho-EGFP-Akt1 remained even after 4 hr. Moreover, control EGFP cells exhibited a dramatic loss of total Akt protein after 2 hr of incubation with H_2O_2, and Akt was no longer detectable after 4 hr. In myr-EGFP-Akt1-transfected cells a drop in Akt1 levels also was detected, but again a significant amount of Akt still was found after 4 hr. In agreement with our previous study, these results suggest that membrane-targeted active Akt is more resistant to H_2O_2-induced dephosphorylation and degradation than the endogenous wild type (Martin et al., 2002). In this experimental frame we analyzed the changes in Cu/Zn-SOD protein levels. As shown in Figure 5, in EGFP cells H_2O_2 induced a slight increase in Cu/Zn-SOD after 1 hr, as expected (Yoo et al., 1999). However, the amount of

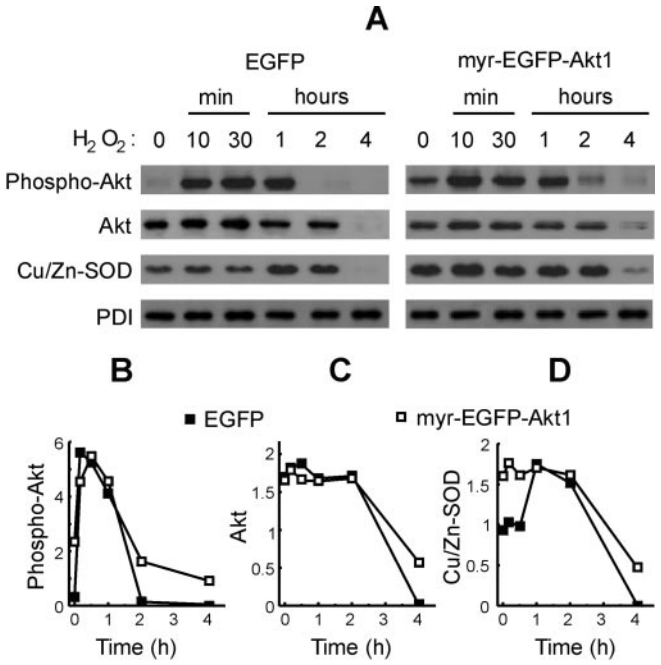

Figure 5. Time course effect of H_2O_2 on Akt and Cu/Zn-SOD protein levels in control EGFP- and myr-EGFP-Akt1-transfected cells. *A*, Cells incubated in low serum for 16 hr were submitted to 0.5 mM H_2O_2 for the indicated times. Top, Immunoblots with anti-phospho-Akt antibodies. Top middle, Immunoblots with anti-Akt antibodies. Bottom middle, Immunoblots with anti-Cu/Zn-SOD antibodies. Bottom, Immunoblots with anti-PDI antibodies of the same lysates showing similar amounts of protein per lane. *B–D*, Densitometric quantitation of phospho-Akt, total Akt, and Cu/Zn-SOD levels relative to PDI levels after treatment with 0.5 mM H_2O_2, as shown in *A*.

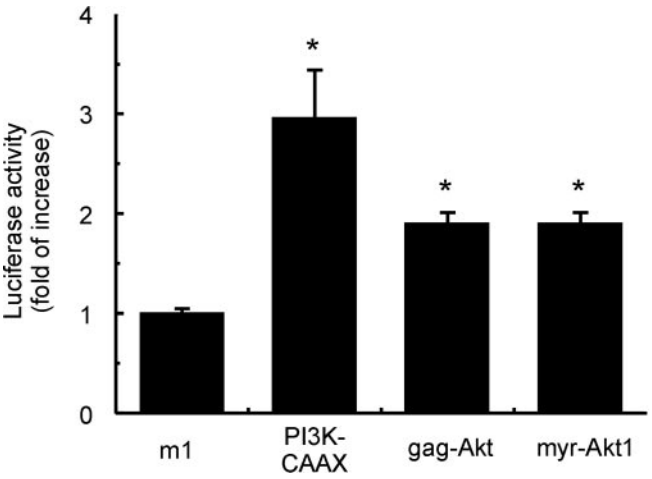

Figure 6. Activation of the human *sod1* promoter by the PI3K/Akt axis. PC12 cells were transiently cotransfected with a luciferase reporter construct containing 1499 bp of the 5′ regulatory sequence of human *sod1* (pGL3basic-*sod1*-1499) and expression vectors for muscarinic receptor m1 as a negative control or for active PI3K-CAAX, gag-Akt, or myr-Akt1. After 24 hr from transfection, the cells were maintained in low serum for 16 hr and then lysed and analyzed for luciferase activity. *$p < 0.001$, comparing m1 versus the other treatments.

Cu/Zn-SOD dropped to undetectable levels after 4 hr. The drop in Cu/Zn-SOD protein levels was prevented by preincubation with the nonselective caspase inhibitor z-Val-Ala-Asp-fluoromethylketone (zVAD-fmk) (data not shown). In contrast, in myr-EGFP-Akt1 cells H_2O_2 did not increase Cu/Zn-SOD levels over the basal ones, which are already high, suggesting that the ectopic expression of active Akt saturated stimulation of Cu/Zn-SOD expression. Moreover, Cu/Zn-SOD levels dropped after long-term incubation with H_2O_2, but, in contrast to control cells, a significant amount still could be detected after 4 hr. Therefore, although these experiments do not demonstrate a causal relationship between regulation of Akt and induction of Cu/Zn-SOD by H_2O_2, they provide a mechanism that may be used, at least in part, by ROS to upregulate Cu/Zn-SOD via activation of Akt (see Discussion).

The regulatory effect of PI3K and Akt on expression of Cu/Zn-SOD also was analyzed by using a luciferase reporter construct carrying the luciferase gene under the control of 1499 bp from the 5′-flanking region of the human *sod1* gene. As shown in Figure 6, cotransfection of this construct with membrane-targeted, active versions of PI3K (PI3K-CAAX) or Akt (myr-Akt1 and gag-Akt) resulted in a two- to threefold increase in luciferase activity over the level of cells cotransfected with a control vector carrying the muscarinic m1 receptor. Taken together, these results indicate that activation of the PI3K/Akt pathway increases the cellular antioxidant capacity at least in part via the upregulation of Cu/Zn-SOD expression.

There are several regulatory elements in the 5′ promoter region of human *sod1* that might be targets of the PI3K/Akt pathway (Fig. 7*A*). To identify these targets, we generated several deletions of the 1499 bp *sod1* promoter and subcloned them into the plasmid pGL3basic to govern luciferase expression. These luciferase reporter constructs were transfected with control vector or with an expression vector for membrane-anchored, active PI3K (PI3K-CAAX). As shown in Figure 7*B*, reporter constructs –1499 to –552 exhibited both basal and PI3K-inducible activity. In contrast, construct –355 exhibited basal activity, but no significant induction by PI3K. The smallest fragments –71 and –29 displayed low basal activity and little or no induction by PI3K. These results indicate the existence of a highly sensitive site for PI3K regulation between –355 and –552 bp of the human *sod1* promoter. As shown in Figure 7*A*, within this region we identified a putative NF-κB-responsive element (analysis by TFsearch software, available at http://www.cbrc.jp/research/db/TFSEARCH.html).

Before the characterization of this site, we first verified the functional activation of NF-κB by the PI3K/Akt signaling pathway in our system in the context of NGF stimulation. Regulation of NF-κB-dependent transcription involves at least two mechanisms (Madrid et al., 2000): (1) modulation of the transactivating domain located in the C-terminal 120 amino acids of p65 and (2) release of transcription factor from the cytoplasmic inhibitor κB (IκB) and subsequent translocation to the nucleus. To analyze whether the PI3K/Akt pathway targets the transactivating domain (TD1) of p65-NF-κB, we used a fusion protein consisting of the p65-NF-κB TD1 and the DNA-binding domain of Gal4. PC12 cells were cotransfected with this expression vector (pGal4-p65) and a reporter plasmid controlling luciferase expression via four Gal4-responsive elements (pGal4-LUC). As shown in Figure 8*A*, in these cells NGF induced luciferase activity by more than twofold. Interestingly, preincubation with the PI3K inhibitor LY294002 significantly attenuated the NGF-induced luciferase expression. In additional experiments we analyzed the regulation of p65-NF-κB transactivation domain 1 in the background of EGFP and myr-EGFP-Akt1 cells. As shown in Figure 8*A*, when cells were cotransfected with pGal4-p65 and pGal4-LUC, we observed that myr-EGFP-Akt1 cells exhibited approximately fourfold more luciferase activity than EGFP cells. These results indicate that NGF regulates NF-κB activity in a PI3K/Akt-dependent manner by a mechanism directed, at least in part, to turn on the transactivation domain of p65-NF-κB. Because regulation of

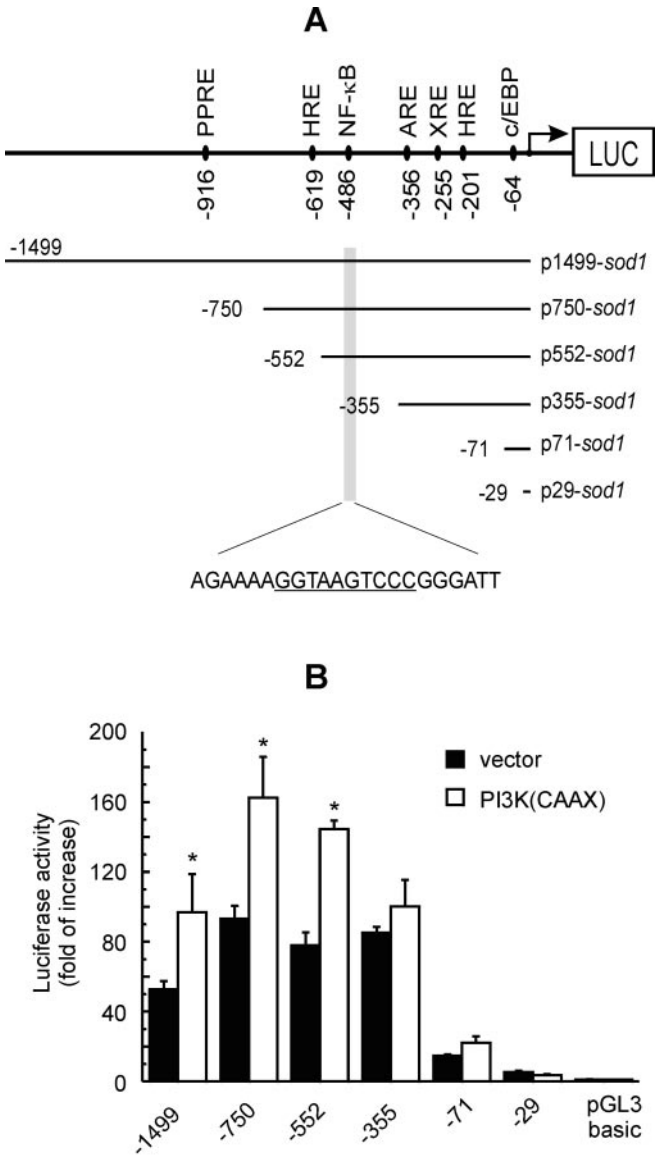

Figure 7. Identification of the *sod1* promoter region that is regulated by PI3K. *A*, Schematic showing candidate regulatory elements for PI3K in the human *sod1* promoter and a detail of a putative NF-κB site at a position between −552 and −355 from the transcription start site. *B*, PC12 cells were cotransfected with an expression vector for active PI3K-CAAX and luciferase reporter constructs containing the indicated fragments of the human *sod1* promoter. After 24 hr from transfection, the cells were maintained in low serum for 16 hr and then lysed and analyzed for luciferase activity. The figure shows folds of increase in luciferase activity over the promoterless vector pGL3basic. *$p < 0.001$, comparing vector-transfected versus PI3K(CAAX)-transfected groups.

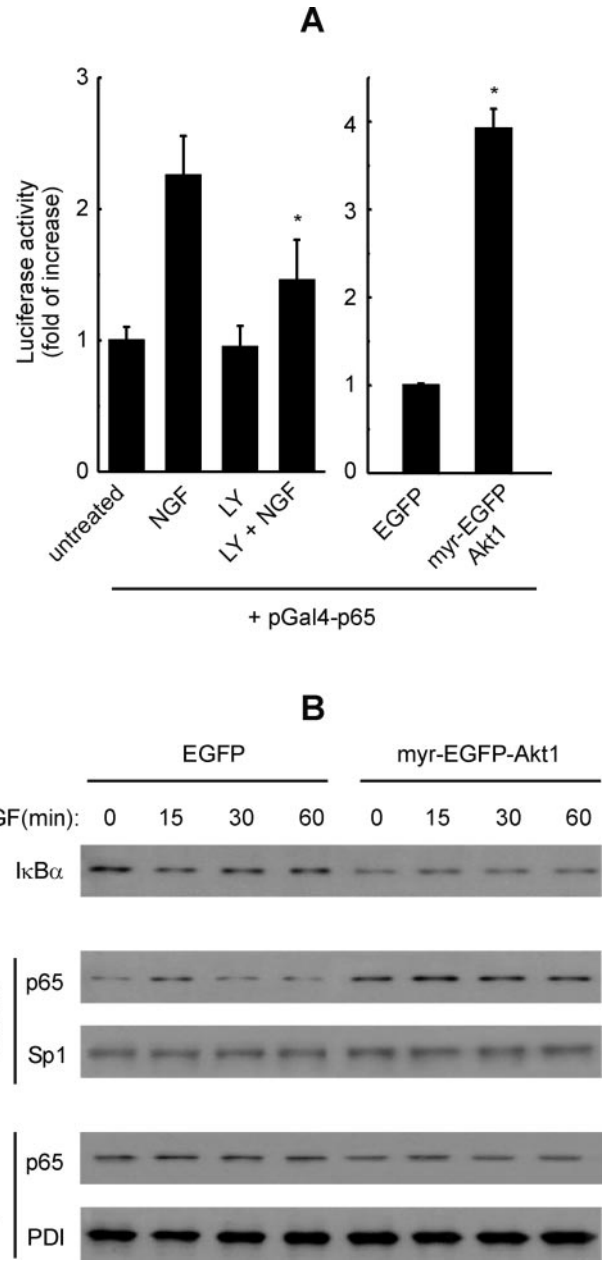

Figure 8. Regulation of NF-κB activity by NGF and Akt signaling. *A*, Effect on the transactivating capacity of p65-NF-κB. Left, PC12 cells were cotransfected with an expression vector for a fusion protein consisting of the transactivation domain of p65-NF-κB and the DNA-binding domain of Gal4 (pGal4-p65) and a luciferase reporter under the control of Gal4 (pGal4-LUC). After 24 hr from transfection, the cells were submitted to low-serum conditions for 16 hr and then pretreated for 15 min with 10 μM LY294002 (LY) or treated with 25 ng/ml NGF for 6 hr, as indicated. Right, EGFP and myr-EGFP-Akt1 cells were cotransfected with the same plasmids (pGal4-p65 and pGal4-LUC), incubated in low serum for 16 hr, and analyzed for luciferase activity. *Statistically significant differences, with $p < 0.001$, comparing NGF-treated groups and EGFP and myr-EGFP-Akt1 groups. *B*, Comparison of the nuclear and cytosolic p65-NF-κB and IκBα protein levels. EGFP and myr-EGFP-Akt1 cells were submitted to low-serum conditions for 16 hr and then stimulated with 25 ng/ml NGF for the indicated times. Cell fractions were resolved in SDS-PAGE and immunoblotted with anti-p65-NF-κB and anti-IκBα antibodies. The same blots were immunoblotted with anti-Sp1 and anti-PDI antibodies to demonstrate similar protein load per lane.

NF-κB also involves nuclear translocation, we compared the nuclear levels of p65-NF-κB after NGF stimulation in control EGFP cells and in myr-EGFP-Akt1 cells. As shown in Figure 8*B*, the basal levels of nuclear p65 were higher and those of cytosolic p65 were slightly lower in myr-EGFP-Akt1 cells as compared with control EGFP cells. Accordingly, basal IκBα levels were slightly lower in myr-EGFP-Akt1 cells. After 15 min of NGF stimulation EGFP cells exhibited a transient increase of nuclear p65-NF-κB, whereas the levels of the housekeeping transcription factor Sp1 were stable. This transient translocation is consistent with observations by other authors (Maggirwar et al., 1998). In contrast, NGF did not alter the distribution of p65-NF-κB in myr-EGFP-Akt1 cells, suggesting either that Akt promotes close to maximal translocation or that Akt plays a substantial role as mediator of NGF-induced regulation of this transcription factor. Interestingly, although control EGFP cells exhibited higher basal IκBα levels than myr-EGFP-Akt1 cells, NGF did not alter these levels

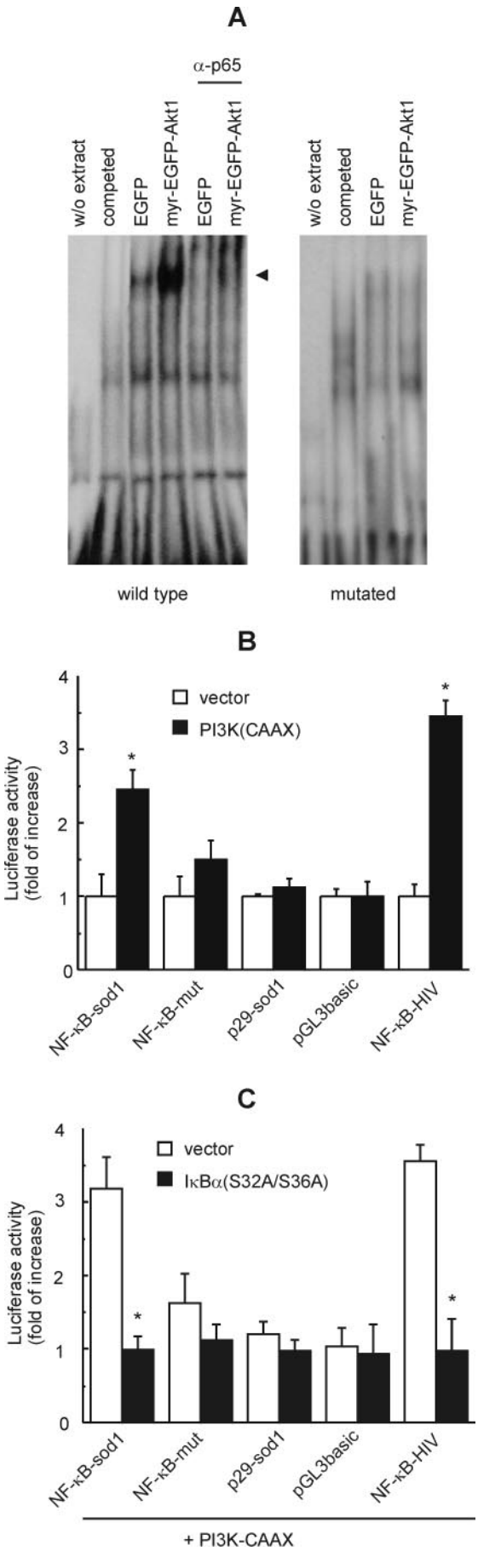

significantly under our experimental conditions, suggesting, in agreement with previous reports (Bui et al., 2001), that NGF induces at least in part the dissociation of p65-NF-κB from the NF-κB/IκB complex by a mechanism that does not necessarily require IκBα degradation (see Discussion).

Taken together, those results indicated that the PI3K/Akt pathway is necessary and sufficient for signaling to NF-κB and provided further support to analyze the regulation of *sod1* via the newly identified NF-κB response element. Therefore, we used electrophoretic mobility shift assays (EMSAs) to determine whether the increase in nuclear p65-NF-κB was sufficient to promote binding of this transcription factor to the putative NF-κB sequence of the human *sod1* promoter. Nuclear extracts from EGFP and myr-EGFP-Akt1 cells were incubated with a ^{32}P-labeled, double-stranded oligonucleotide comprising three tandem copies of the putative *sod1* NF-κB sequence or a similar probe mutated to abolish NF-κB binding (see Materials and Methods). As shown in Figure 9*A*, among the several retarded complexes formed with the NF-κB probe, one of them was barely detectable in the mutated probe. In addition, the intensity of this retarded band was increased significantly in the myr-EGFP-Akt1 nuclear extracts as compared with the EGFP ones. Moreover, when an antibody against p65-NF-κB was included in the binding reaction, the intensity of this retarded band decreased dramatically, indicating the presence of p65-NF-κB in the complex. These results support the existence of a p65-NF-κB binding site in this region of the *sod1* promoter and its upregulation by the PI3K/Akt pathway.

Finally, to analyze the functional regulation of the NF-κB binding site of *sod1* by the PI3K/Akt pathway, we generated two luciferase reporter constructs containing three wild-type (NF-κB-*sod1*) or three mutated (NF-κB-*mut*) sequences of the 10 bp corresponding to the putative NF-κB regulatory element of human *sod1* and linked them to the –29 luciferase *sod1* reporter construct. As a positive control of NF-κB regulation, we also analyzed the promoter activity of a well established NF-κB regulatory sequence from human immunodeficiency virus (NF-κB-HIV). As shown in Figure 9*B*, PC12 cells cotransfected with active PI3K-CAAX and either NF-κB-*sod1* or NF-κB-HIV induced an approximately threefold increase in luciferase activity over the level of cells cotransfected with empty vector. In contrast, cells cotransfected with NF-κB-*mut*, p29-*sod1*, or pGL3basic yielded similar luciferase activity in the presence of PI3K-CAAX or empty vector. To demonstrate further a role of NF-κB as a mediator of PI3K regulation for this site, we used a dominant-negative mutant of the inhibitor of NF-κB, IκBα(S32A/S36A). This mutant

←

Figure 9. The NF-κB site is sufficient to confer PI3K inducibility to the human *sod1* promoter. *A*, EMSA, using a double-stranded oligonucleotide with the putative NF-κB sequence (wild type) identified in the human *sod1* promoter or a mutated control sequence (mutated) and nuclear extracts from PC12 cells expressing EGFP or myr-EGFP-Akt1. The arrow points to the position of a band that was not formed when the complexes were incubated in the presence of anti-p65-NF-κB antibody. *B*, Luciferase activity of PC12 cells cotransfected with PI3K-CAAX or empty vector and reporter constructs comprising three wild-type tandem or three mutated tandem sequences for the NF-κB site of human *sod1*. In addition, the cells also were cotransfected with a luciferase reporter construct for NF-κB from human immunodeficiency virus (NF-κB-HIV), with p29-*sod1*, or with pGL3basic. *$p < 0.001$, comparing vector-transfected versus PI3K(CAAX)-transfected groups. *C*, Blockage of PI3K induction of the NF-κB-responsive element by cotransfection with dominant-negative IκBα(S32A/S36A) mutant. Cells were cotransfected as in *B* plus the expression vector for IκBα(S32A/S36A). After 24 hr from transfection, the cells were submitted to low-serum conditions for 16 hr and then analyzed for luciferase activity. *$p <$ 0.001, comparing vector-transfected versus IκBα(S32A/S36A)-transfected groups.

contains two substitutions (S32A and S36A) that prevent its phosphorylation and subsequent proteasomal degradation, therefore exhibiting permanent sequestration of NF-κB (Traenckner et al., 1995). As shown in Figure 9*C*, IκBα(S32A/S36A) blocked the PI3K-CAAX-mediated increase both in NF-κB-HIV and in NF-κB-*sod1* activities and did not have a significant inhibitory effect on the activities of NF-κB-*mut*, p29-*sod1*, and pGL3basic. Taken together, these results indicate that the PI3K/Akt pathway increases the cellular antioxidant defense at least in part via the upregulation of Cu/Zn-SOD expression at the level of the newly identified NF-κB regulatory site.

Discussion

In this study we present evidence that the PI3K/Akt survival pathway is involved in protection against oxidative damage by increasing the expression of Cu/Zn-SOD. Cells expressing active Akt1 kinase exhibited lower ROS levels in response to H_2O_2 and higher mRNA and protein levels of Cu/Zn-SOD. In addition to the regulation of Cu/Zn-SOD, we also observed mRNA and protein accumulation of other antioxidant enzymes, including Mn-SOD (data not shown) and heme oxygenase-1 (Salinas et al., 2003; Martin et al., 2004) in cells with an active PI3K/Akt pathway. Of note, several groups including ours have reported the activation of Akt in response to oxidative stress in a PI3K-dependent manner (Konishi et al., 1997; Shaw et al., 1998; Martin et al., 2002). According to these observations, it is tempting to consider the PI3K/Akt axis as a sensor for intracellular ROS levels that maintains ROS homeostasis via transcriptional activation of antioxidant enzymes.

Activation of Akt by H_2O_2 correlated with an increase in Cu/Zn-SOD levels. However, when cells were pretreated with the PI3K inhibitor LY294002, we did not detect a decrease in Cu/Zn-SOD expression (data not shown). Therefore, H_2O_2 induces *sod1* via several overlapping mechanisms that may be Akt-dependent and -independent. For instance, Yoo et al. (1999) have reported the regulation of *sod1* promoter by H_2O_2 at the level of hydrogen peroxide-responsive (PPRE) and heat shock (HSE) elements. These results illustrate (as shown in Fig. 7*A*) the complex transcriptional regulation of this gene that probably involves multiple positive and negative regulatory elements acting in concert.

Previous studies have reported the upregulation of Cu/Zn-SOD in response to growth factors and neurotrophins (Kong et al., 1993; Yoo et al., 1999; Chang et al., 2002; Park and Rho, 2002). Our results also suggest that *sod1* is subjected to NGF control via PI3K/Akt/NF-κB signaling. Here we report for the first time the functional characterization of one NF-κB site in human *sod1* and, most importantly, its regulation by the PI3K/Akt pathway. The identified sequence starts at position −486 and binds p65-NF-κB. Moreover, NGF activated the transactivation domain of p65-NF-κB in a PI3K/Akt-dependent manner and also produced a transient translocation of this transcription factor to the nucleus, therefore providing a mechanism to explain how Akt1 upregulates Cu/Zn-SOD expression. The relevance of NF-κB on the PI3K/Akt1-mediated regulation of Cu/Zn-SOD expression was demonstrated further by the fact that a dominant-negative IκBα mutant prevented the *sod1* promoter activation by PI3K-CAAX. Interestingly, when we analyzed Cu/Zn-SOD protein levels after NGF stimulation, we could detect barely a small increase after 4 hr of treatment (data not shown). Although we do not have a conclusive explanation for this discrepancy, we suggest that regulation of *sod1* expression is submitted to an exquisite homeostatic control via positive and negative regulatory elements, and, therefore, NGF-induced stimulation requires either a very strong/persistent activation of the PI3K/Akt pathway or cooperation with other factors.

The regulation of NF-κB by cytokine signaling, such as tumor necrosis factor-α (TNF-α), has been established in detail (Hoffmann et al., 2002). The current model indicates that, under non-stimulated conditions, p65-NF-κB is sequestered in the cytoplasm via association with protein inhibitors of κB (IκB). Cytokine stimulation promotes IκBα phosphorylation at serine residue 32 by specific kinases (IKK) and subsequent targeting for degradation by the ubiquitin–proteasome pathway. Therefore, this model provides a mechanism for translocation of p65-NF-κB to the nucleus and heterodimerization with other NF-κB members for transcriptional regulation. However, the regulation of NF-κB activity by NGF and by Akt remains controversial. For instance, Madrid et al. (2000) reported that Akt stimulates the transactivation potential but barely increases the nuclear translocation of p65-NF-κB in HEK 293T cells. Regarding NGF, Bui et al. (2001) reported the NGF-induced dissociation of the cytosolic p65/IκBα complex via phosphorylation of IκBα at tyrosine residue 42. Contrary to cytokine model, this mechanism results in nuclear translocation of p65-NF-κB without significant degradation of IκBα. On the other hand, Maggirwar et al. (1998) described that NGF-induced NF-κB contains heteromeric complexes of p65 and p50 members and that NGF induces degradation of IκBα, which is prevented by proteasome inhibitors. The discrepancies among these studies may be related in part to cell type specificity and methodological differences. For instance, the Maggirwar study reported the partial degradation of IκBα in cells isotopically labeled with ^{35}S-methionine. In agreement with this, we have observed a substantial decrease in IκBα levels in cells submitted to the protein synthesis inhibitor cycloheximide (data not shown). However, the studies that relied on direct immunoblot detection of total IκBα might have missed this observation because the expression of IκBα is upregulated by NF-κB as a negative feedback loop (Hoffmann et al., 2002), and, therefore, the change in IκBα levels is very transient in NGF-treated cells. The low rate of NGF-induced degradation of IκBα in comparison to that of TNF-α may argue against the relevance of such degradation in this scenario. In any case, our results in PC12 cells indicate that NGF induces the transactivating activity of p65-NF-κB in a PI3K-dependent manner and also induces its transient nuclear translocation by a mechanism that requires little or no contribution of IκBα degradation. In addition, the persistent Akt activation also results in a sustained increase of nuclear p65-NF-κB and a decrease of IκBα protein levels. Finally, our results are in agreement with all of the above mentioned studies in the observation that increased IκBα levels prevent activation of p65-NF-κB by Akt because the dominant-negative mutant IκBα(S32A/S36A) substantially attenuated Akt-mediated activation of the NF-KB regulatory site identified in the human *sod1*.

In the 5′-flanking region of human *sod1* there are several putative binding sites for transcription factors that are regulated by phosphorylation and might be targets of PI3K and Akt. These include a CCAAT/enhancer binding protein (c/EBP), HSE, XRE, ARE NF-κB, and PPRE. Although some of these sites have been studied in detail (Minc et al., 1999; Yoo et al., 1999; Chang et al., 2002; Park and Rho, 2002), the regulation by NF-κB has remained unexplored. However, this site remains particularly attractive to study the regulation of Cu/Zn-SOD because NF-κB family members are controlled by cell redox status and are involved in cell survival (Mattson and Camandola, 2001; Karin and Lin, 2002; Wang et al., 2002; Storz and Toker, 2003). Therefore,

the upregulation of the antioxidant enzyme Cu/Zn-SOD by the PI3K/Akt axis provides a connection between a transcription factor sensitive to redox regulation, such as NF-κB, and a survival pathway, represented by the PI3K and Akt.

Contrary to the observations reported in this study, Honda and Honda (2002) have reported in *Caenorhabditis elegans* that the absence of PI3K/Akt signaling results in activation of the Forkhead transcription factor homolog DAF-16 and causes the dauer phenotype, characterized by low metabolic rate and increased resistance to oxidative stress. From consistent studies in mammalian cells, Kops et al. (2002) have suggested that Akt and Forkhead transcription factors of the FOXO family might exert complementary functions in proliferating and quiescent cells. In agreement with this hypothesis, we suggest that the PI3K/Akt axis inversely regulates the subcellular distribution of NF-κB and FOXO transcription factors to adapt the level of antioxidant enzymes to specific metabolic situations. In the presence of neurotrophins, growth factors, or oxidative stress the activation of Akt results in the direct phosphorylation of FOXO factors, causing their displacement from the nucleus into the cytoplasm. Simultaneously, Akt induces translocation of NF-κB to the nucleus and activation of antioxidant genes. On the contrary, in quiescent cells, where Akt is not active, most of NF-κB is sequestered into the cytoplasm while nonphosphorylated active FOXO transcription factors localize to the nucleus and guard the proper expression of antioxidant genes. Together with Mn-SOD (Kops et al., 2002), Cu/Zn-SOD might be included among the antioxidant enzymes subjected to dual regulation by the pair NF-κB/FOXO because, in addition to the control exerted by PI3K/Akt/NF-κB, we have identified putative sites of regulation by Forkhead transcription factors in the human *sod1* gene (starting at positions –1376, –1231, and –822) that might be targets of FOXO members under quiescent conditions.

Oxidative stress has been implicated in the neuronal cell death of several neurodegenerative diseases such as Alzheimer's and Parkinson's diseases. Strategies aimed to prevent the increase in ROS during the course of these disorders may attenuate or stop neuronal death and therefore may have significant clinical utility. This study suggests that activation of the PI3K/Akt/NF-κB pathway might reinforce the antioxidant cell capacity and provide protection against oxidant damage via the upregulation of antioxidant genes such as *sod1*.

References

Asanuma M, Hirata H, Cadet JL (1998) Attenuation of 6-hydroxydopamine-induced dopaminergic nigrostriatal lesions in superoxide dismutase transgenic mice. Neuroscience 85:907–917.

Bindokas VP, Jordán J, Lee CC, Miller RJ (1996) Superoxide production in rat hippocampal neurons: selective imaging with hydroethidine. J Neurosci 16:1324–1336.

Brunet A, Bonni A, Zigmond MJ, Lin MZ, Juo P, Hu LS, Anderson MJ, Arden KC, Blenis J, Greenberg ME (1999) Akt promotes cell survival by phosphorylating and inhibiting a Forkhead transcription factor. Cell 96:857–868.

Brunet A, Datta SR, Greenberg ME (2001) Transcription-dependent and -independent control of neuronal survival by the PI3K-Akt signaling pathway. Curr Opin Neurobiol 11:297–305.

Bui NT, Livolsi A, Peyron JF, Prehn JH (2001) Activation of nuclear factor-κB and *bcl-x* survival gene expression by nerve growth factor requires tyrosine phosphorylation of IκBα. J Cell Biol 152:753–764.

Chan PH, Kawase M, Murakami K, Chen SF, Li Y, Calagui B, Reola L, Carlson E, Epstein CJ (1998) Overexpression of SOD1 in transgenic rats protects vulnerable neurons against ischemic damage after global cerebral ischemia and reperfusion. J Neurosci 18:8292–8299.

Chang MS, Yoo HY, Rho HM (2002) Transcriptional regulation and environmental induction of gene encoding copper- and zinc-containing superoxide dismutase. Methods Enzymol 349:293–305.

Du K, Montminy M (1998) CREB is a regulatory target for the protein kinase Akt/PKB. J Biol Chem 273:32377–32379.

Franke TF, Hornik CP, Segev L, Shostak GA, Sugimoto C (2003) PI3K/Akt and apoptosis: size matters. Oncogene 22:8983–8998.

Fridovich I (1997) Superoxide anion radical ($O^{\cdot}_2$), superoxide dismutases, and related matters. J Biol Chem 272:18515–18517.

Fridovich I (1999) Fundamental aspects of reactive oxygen species, or what's the matter with oxygen? Ann NY Acad Sci 893:13–18.

Hasper HJ, Weghorst RM, Richel DJ, Meerwaldt JH, Olthuis FM, Schenkeveld CE (2000) A new four-color flow cytometric assay to detect apoptosis in lymphocyte subsets of cultured peripheral blood cells. Cytometry 40:167–171.

Hoffmann A, Levchenko A, Scott ML, Baltimore D (2002) The IκB-NF-κB signaling module: temporal control and selective gene activation. Science 298:1241–1245.

Honda Y, Honda S (2002) Oxidative stress and life span determination in the nematode *Caenorhabditis elegans*. Ann NY Acad Sci 959:466–474.

Kane LP, Shapiro VS, Stokoe D, Weiss A (1999) Induction of NF-κB by the Akt/PKB kinase. Curr Biol 9:601–604.

Karin M, Lin A (2002) NF-κB at the crossroads of life and death. Nat Immunol 3:221–227.

Klein JA, Ackerman SL (2003) Oxidative stress, cell cycle, and neurodegeneration. J Clin Invest 111:785–793.

Kong XJ, Lee SL, Lanzillo JJ, Fanburg BL (1993) Cu, Zn superoxide dismutase in vascular cells: changes during cell cycling and exposure to hyperoxia. Am J Physiol 264:L365–L375.

Konishi H, Matsuzaki H, Tanaka M, Takemura Y, Kuroda S, Ono Y, Kikkawa U (1997) Activation of protein kinase B (Akt/RAC-protein kinase) by cellular stress and its association with heat shock protein Hsp27. FEBS Lett 410:493–498.

Kops GJ, Dansen TB, Polderman PE, Saarloos I, Wirtz KW, Coffer PJ, Huang TT, Bos JL, Medema RH, Burgering BM (2002) Forkhead transcription factor FOXO3a protects quiescent cells from oxidative stress. Nature 419:316–321.

Kunikowska G, Jenner P (2003) Alterations in m-RNA expression for Cu, Zn-superoxide dismutase and glutathione peroxidase in the basal ganglia of MPTP-treated marmosets and patients with Parkinson's disease. Brain Res 968:206–218.

Kuruvilla R, Ye H, Ginty DD (2000) Spatially and functionally distinct roles of the PI3-K effector pathway during NGF signaling in sympathetic neurons. Neuron 27:499–512.

Littlewood TD, Hancock DC, Danielian PS, Parker MG, Evan GI (1995) A modified estrogen receptor ligand-binding domain as an improved switch for the regulation of heterologous proteins. Nucleic Acids Res 23:1686–1690.

Madrid LV, Wang CY, Guttridge DC, Schottelius AJ, Baldwin Jr AS, Mayo MW (2000) Akt suppresses apoptosis by stimulating the transactivation potential of the RelA/p65 subunit of NF-κB. Mol Cell Biol 20:1626–1638.

Maggirwar SB, Sarmiere PD, Dewhurst S, Freeman RS (1998) Nerve growth factor-dependent activation of NF-κB contributes to survival of sympathetic neurons. J Neurosci 18:10356–10365.

Martin D, Salinas M, Lopez-Valdaliso R, Serrano E, Recuero M, Cuadrado A (2001) Effect of the Alzheimer amyloid fragment $A\beta_{25-35}$ on Akt/PKB kinase and survival of PC12 cells. J Neurochem 78:1000–1008.

Martin D, Salinas M, Fujita N, Tsuruo T, Cuadrado A (2002) Ceramide and reactive oxygen species generated by H_2O_2 induce caspase-3-independent degradation of Akt/protein kinase B. J Biol Chem 277:42943–42952.

Martin D, Rojo AI, Salinas M, Diaz R, Gallardo G, Alam J, Ruiz de Galarreta CM, Cuadrado A (2004) Regulation of heme oxygenase-1 expression through the phosphatidylinositol 3 kinase/Akt pathway and the Nrf2 transcription factor in response to the antioxidant phytochemical carnosol. J Biol Chem 279:8919–8929.

Mattson MP, Camandola S (2001) NF-κB in neuronal plasticity and neurodegenerative disorders. J Clin Invest 107:247–254.

Minc E, de Coppet P, Masson P, Thiery L, Dutertre S, Amor-Gueret M, Jaulin C (1999) The human copper-zinc superoxide dismutase gene (SOD1) proximal promoter is regulated by Sp1, Egr-1, and WT1 via non-canonical binding sites. J Biol Chem 274:503–509.

Montaner S, Perona R, Saniger L, Lacal JC (1999) Activation of serum re-

sponse factor by RhoA is mediated by the nuclear factor-κB and C/EBP transcription factors. J Biol Chem 274:8506–8515.

Park EY, Rho HM (2002) The transcriptional activation of the human copper/zinc superoxide dismutase gene by 2,3,7,8-tetrachlorodibenzo-*p*-dioxin through two different regulator sites, the antioxidant responsive element and xenobiotic responsive element. Mol Cell Biochem 240:47–55.

Salinas M, Lopez-Valdaliso R, Martin D, Alvarez A, Cuadrado A (2000) Inhibition of PKB/Akt1 by C2-ceramide involves activation of ceramide-activated protein phosphatase in PC12 cells. Mol Cell Neurosci 15:156–169.

Salinas M, Martin D, Alvarez A, Cuadrado A (2001) Akt1/PKBα protects PC12 cells against the parkinsonism-inducing neurotoxin 1-methyl-4-phenylpyridinium and reduces the levels of oxygen-free radicals. Mol Cell Neurosci 17:67–77.

Salinas M, Diaz R, Abraham NG, Ruiz de Galarreta CM, Cuadrado A (2003) Nerve growth factor protects against 6-hydroxydopamine-induced oxidative stress by increasing expression of heme oxygenase-1 in a phosphatidylinositol 3-kinase-dependent manner. J Biol Chem 278:13898–13904.

Shaw M, Cohen P, Alessi DR (1998) The activation of protein kinase B by H_2O_2 or heat shock is mediated by phosphoinositide 3-kinase and not by mitogen-activated protein kinase-activated protein kinase-2. Biochem J 336:241–246.

Storz P, Toker A (2003) NF-κB signaling—an alternate pathway for oxidative stress responses. Cell Cycle 2:9–10.

Takeuchi A, Miyaishi O, Kiuchi K, Isobe K (2000) Cu/Zn- and Mn-superoxide dismutases are specifically up-regulated in neurons after focal brain injury. J Neurobiol 45:39–46.

Traenckner EB, Pahl HL, Henkel T, Schmidt KN, Wilk S, Baeuerle PA (1995) Phosphorylation of human IκB-α on serines 32 and 36 controls IκB-α proteolysis and NF-κB activation in response to diverse stimuli. EMBO J 14:2876–2883.

Wang T, Zhang X, Li JJ (2002) The role of NF-κB in the regulation of cell stress responses. Int Immunopharmacol 2:1509–1520.

Yoo HY, Chang MS, Rho HM (1999) The activation of the rat copper/zinc superoxide dismutase gene by hydrogen peroxide through the hydrogen peroxide-responsive element and by paraquat and heat shock through the same heat shock element. J Biol Chem 274:23887–23892.

Zelko IN, Mariani TJ, Folz RJ (2002) Superoxide dismutase multigene family: a comparison of the Cu/Zn-SOD (SOD1), Mn-SOD (SOD2), and EC-SOD (SOD3) gene structures, evolution, and expression. Free Radic Biol Med 33:337–349.